ISSN 1674-1056
http://cpb.iphy.ac.cn
http://iopscience.iop.org/cpb
中国物理 B
Chinese Physics
中国物理 Chinese Physics B

Forbidden transition properties of fine-structure $2p^3\ ^4S_{3/2}$-$2p^3\ ^2D_{3/2,5/2}$ for nitrogen-like ions

Xiao-Kang He(何晓康), Jian-Peng Liu(刘建鹏), Xiang Zhang(张祥), Yong Shen(沈咏), Hong-Xin Zou(邹宏新)
Citation: Chin. Phys. B . 2018, 27(8): 083102. **doi:** 10.1088/1674-1056/27/8/083102

Journal homepage: http://cpb.iphy.ac.cn; http://iopscience.iop.org/cpb

What follows is a list of articles you may be interested in

Uncertainty evaluation of the isotope shift factors for $2s2p^{3,1}P_1^o$-$2s^{21}S_0$ transitions in B II

Jianpeng Liu(刘建鹏), Jiguang Li(李冀光), Hongxin Zou(邹宏新)
Chin. Phys. B . 2017, 26(2): 023104. **doi:** 10.1088/1674-1056/26/2/023104

Low-lying electronic states of CuN calculated by MRCI method

Shu-Dong Zhang(张树东), Chao Liu(刘超)
Chin. Phys. B . 2016, 25(10): 103103. **doi:** 10.1088/1674-1056/25/10/103103

Configuration interaction studies on the spectroscopic properties of PbO including spin—orbit coupling

Wang Luo(罗旺), Rui Li(李瑞), Zhiqiang Gai(盖志强), RuiBo Ai(艾瑞波), Hongmin Zhang(张宏民), Xiaomei Zhang(张晓美), Bing Yan(闫冰)
Chin. Phys. B . 2016, 25(7): 073101. **doi:** 10.1088/1674-1056/25/7/073101

Accurate spectroscopic constants of the lowest two electronic states in S_2 molecule with explicitly correlated method

Changli Wei(魏长立), Xiaomei Zhang(张晓美), Dajun Ding(丁大军), Bing Yan(闫冰)
Chin. Phys. B . 2016, 25(1): 013102. **doi:** 10.1088/1674-1056/25/1/013102

Weak- and hyperfine-interaction-induced 1s2s $^1S_0 \rightarrow 1s^2\ ^1S_0$ E1 transition rates of He-like ions

Laima Radžiūtė, Erikas Gaidamauskas, Gediminas Gaigalas, Li Ji-Guang, Dong Chen-Zhong, Per Jönsson
Chin. Phys. B . 2015, 24(4): 043103. **doi:** 10.1088/1674-1056/24/4/043103

Forbidden transition properties of fine-structure $2p^3\ ^4S_{3/2}$–$2p^3\ ^2D_{3/2,5/2}$ for nitrogen-like ions*

Xiao-Kang He(何晓康), Jian-Peng Liu(刘建鹏), Xiang Zhang(张祥), Yong Shen(沈咏), and Hong-Xin Zou(邹宏新)†

College of Liberal Arts and Sciences, National University of Defense Technology, Changsha 410073, *China*

(Received 10 March 2018; revised manuscript received 9 May 2018; published online 10 July 2018)

Based on relativistic wave functions from multiconfiguration Dirac–Hartree–Fock and configuration interaction calculations, E2 and M1 transition probabilities of $2p^3\ ^4S_{3/2}$–$2p^3\ ^2D_{3/2,5/2}$ are investigated in the nitrogen-like sequence with $7 \leq Z \leq 16$. The contributions of the electron correlations, Breit interaction, and the quantum electrodynamic (QED) effects on the transition properties are analyzed. The present results can be used for diagnosing plasma. In addition, several N-like ions can also be recommended as a promising candidate for a highly charged ion (HCI) clock with a quality factor (Q) of transition as high as 10^{20}.

Keywords: forbidden transition probabilities, nitrogen-like ions, MCDHF method, RCI

PACS: 31.15.V–, 31.15.ve, 31.15.vj, 32.70.Cs **DOI:** 10.1088/1674-1056/27/8/083102

1. Introduction

Optical frequency standard has truly made impressive advances over the past decade. Presently lattice clocks have demonstrated a stability at the 10^{-18} level (Yb,[1] Sr[2]). Such a high precision has a profound influence on testing the spatiotemporal variation of fundamental constants and searching for dark matter. It is also expected to replace the cesium fountain clock to define the international unit "second". However, an optical clock is very sensitive to environmental perturbations and the blackbody radiation (BBR), electric quadrupole frequency shift, Zeeman shifts in a magnetic field, ac-Stark shifts induced by laser, etc., all of which will contribute to the uncertainty of the "Clock". Fortunately, the new generation of nucleus clocks and highly charged ion (HCI) clocks are much less affected by these factors. ^{229}Th nuclear clock utilizing the environment-resistant neutron transition in nucleus is estimated to have a fractional accuracy at the 10^{-19} level.[3] Since the neutron is tightly wrapped in the nucleus, the transition is hardly affected by external factors. Like the nuclear clock, the electron cloud of HCIs has a shrunken size, which causes a small frequency uncertainty with an accuracy below 10^{-19}.[4] The breakthrough of quantum-logic spectroscopy, sympathetic laser cooling, and ion crystal trapping techniques[5] has provided a possibility to realize this kind of new ultra-precise optical frequency standard. It has become an urgent task to find candidates that are easy to realize experimentally and have high quality factors and low uncertainty. Yudin[6] estimated the magnetic-dipole (M1) transitions in HCIs with a single s-valence electron, a single p-valence electron, and two p-valence shell electrons, which can be considered as high-accuracy candidates for HCIs clocks. Yu[7] have investigated M1 transitions in the Al-like $^{51}V^{10+}$, $^{53}Cr^{11+}$, $^{55}Mn^{12+}$, $^{57}Fe^{13+}$, $^{59}Co^{14+}$, $^{61}Ni^{15+}$, and $^{63}Cu^{16+}$ ions as possible clock frequency standards. Liu[8] recommended Cu^{10+} and Zn^{11+} as candidates for HCI clocks. In this paper, we propose that HCI with three p-valence shell electrons (nitrogen-like sequence) be the candidate. In addition, the transition spectrum also has an important application in plasma diagnosis. Some transitions for the N-like ions falling in the UV spectral range have been observed by the SOHO/SUMER instrument in the solar spectrum, which plays an important role in the study of solar internal activity.[9]

Owing to the importance in astrophysics and plasma physics, a lot of theoretical and experimental researches on the nitrogen-like sequence have been performed in recent years. Edlén[10,11] observed the transition spectra among the configurations $2s^22p^3$, $2s2p^4$, and $2p^5$ of the nitrogen-like sequence in tokamak plasma, and he derived and recommended the level values for ions in a range of $Z = 10$–36 by comparing with the corresponding theoretical values from the tables of Cheng.[12] Recently, the transitions of $2s^22p^3$–$2s2p^4$ in nitrogen-like tungsten ion have been measured by electron beam ion traps (EBITs).[13] Träbertet[14,15] measured the lifetime of the $2s^22p^3\ ^2P_{1/2,3/2}$ levels of S X in a heavy-ion storage ring, while the lifetime of highly ionized silicon was measured by using beam-foil spectroscopy.

With the development of the theoretical methods in atomic physics and the capacity of computers, nitrogen-like sequences have been widely studied. Zeippen,[16,17] Becker,[18] and Godefroid[19] successively gave the computing results using the multiconfiguration Hartree–Fock method with relativistic corrections in the Breit–Pauli approximation

*Project supported by the National Natural Science Foundation of China (Grant Nos. 11604385 and 91436103).

†Corresponding author. E-mail: hxzou@nudt.edu.cn

© 2018 Chinese Physical Society and IOP Publishing Ltd

(MCHF-BP). Merkelis[20] used second-order many-body perturbation theory (MBPT) with relativistic corrections in the Breit-Pauli approximation to calculate the transitions of ions in a range of $Z = 10$–30. Using relativistic multi-reference Møller–Plesset perturbation theory (MRMP), Vilkas[21] calculated the energy levels and transition probabilities of some nitrogen-like ion sequences. Froese Fischer and Tachiev[22,23] published their analysis of fine structure splitting and transition rates for the ground configuration in the nitrogen-like sequence up to Zn XXIV using the multiconfiguration Hartree–Fock with relativistic corrections in the Breit-Pauli approximation (MCHF-BP), which has become an authoritative reference for others. Wang[24] used the multiconfiguration Dirac–Hartree–Fock self-consistent field method and the relativistic configuration interaction method (MCDHF + RCI) with quantum electrodynamics corrections to calculate the fine-structure energy levels of the ground-state configuration up to $Z = 22$. The influence of Breit interaction together with the quantum electrodynamic (QED) effects for level splittings was also analyzed in the work. With the same method, Rynkun[25] evaluated E1, M1, E2, and M2 transition rates, weighted oscillator strengths, and lifetimes for the states of the $2s^2 2p^3$, $2s2p^4$, and $2p^5$ configurations in all nitrogen-like ions between F^{3+} and Kr^{30+} but did not present the forbidden transition rates $2p^3\ ^4S_{3/2}$–$2p^3\ ^2D_{3/2,5/2}$. Focusing on the scaling law, Han[26] calculated transition probabilities in $2p^3$ configuration of a nitrogen-like sequence with $7 \le Z \le 79$. Neither the high order correlation effect or the QED effect in the calculation was taken into account. In the database of NIST, most of forbidden transition rates $2p^3\ ^4S_{3/2}$–$2p^3\ ^2D_{3/2,5/2}$ are theoretical data cited from Zeippen,[17] Merkelis,[20] Froese Fischer and Tachiev.[22,23] The data of Ne^{4+} were given by Garstang in 1960,[27] while F^{3+} and P^{9+} data were cited from Naqvi' working in 1951.[28]

In this paper, based on relativistic wave functions from multiconfiguration Dirac–Hartree–Fock and configuration interaction calculations, E2 and M1 transition probabilities of $2p^3\ ^4S_{3/2}$–$2p^3\ ^2D_{3/2,5/2}$ are investigated in the nitrogen-like sequence with $7 \le Z \le 16$. The contributions of the electron correlations, Breit interaction, and the quantum electrodynamic effect are analyzed. The calculation results show the Q factor goes up to 10^{20}, and we recommend F^{2+}, Ne^{3+}, and Na^{4+} as the candidates for the HCI clocks.

2. Theory and computational details

2.1. MCDHF method, RCI method, and transition parameters

The multiconfiguration Dirac–Hartree–Fock method was used in the present work. The Dirac–Coulomb Hamiltonian has the form as

$$H_{\rm DC} = \sum_{i=1}^{N} \left(c\boldsymbol{\alpha}_i \cdot \boldsymbol{p}_i + (\beta_i - 1)c^2 + V_i^N \right) + \sum_{i>j}^{N} \frac{1}{r_{ij}}, \tag{1}$$

where V_i^N is the monopole part of the electron–nucleus Coulomb interaction, α and β are the 4×4 Dirac matrices, and c is the speed of light.

The atomic state function (ASF) was obtained as a linear combination of symmetry adapted configuration state functions (CSFs) with the same parity P, the total angular momentum J, and its projection along the z direction M_J, which is written as

$$\Psi(\gamma PJM_J) = \sum_{j=1}^{\rm NCSFs} c_j \Phi(\gamma_j PJM_J). \tag{2}$$

Here, NCSFs is the number of CSFs, c_j is the mixing coefficient of the corresponding CSF, and γ_j is the additional appropriate labeling of the state j. CSFs are formed by products of one-electron Dirac orbitals. Based on a weighted energy average of several states, the so-called extended optimal level (EOL) scheme, both the radial parts of the Dirac orbitals and the expansion coefficients were optimized to be self-consistent in the relativistic self-consistent field (SCF) procedure.

In subsequent relativistic configuration interaction (RCI) calculations, the transverse photon interaction (Breit interaction) was included in the Hamiltonian, while c_j could be optimized. The Breit interaction in the low-frequency approximation ($\omega_{ij} \to 0$) is taken into account in the procedure, which has the following form:

$$H_{\rm Breit} = -\frac{1}{2r_{ij}} \left[\boldsymbol{\alpha} i \cdot \boldsymbol{\alpha}_j + \frac{(\boldsymbol{\alpha} i \cdot \boldsymbol{r}_{ij})(\boldsymbol{\alpha} j \cdot \boldsymbol{r}_{ij})}{r_{ij}^2} \right]. \tag{3}$$

The leading quantum electrodynamics (QED) corrections, the self-energy, and the vacuum polarization, are also included in the diagonal elements of the Hamiltonian (details can be found in Ref. [29]). Using the self-energy in a hydrogenlike system, a rough estimate of the self-energy in GRASP is obtained by setting

$$H_{rr}^{\rm SE} = \sum_{a=1}^{n_w} q_r(a) E_{n_a\kappa_a}^{\rm SE},$$
$$E_{n_a\kappa_a}^{\rm SE} = \frac{\left(Z_a^{\rm eff}\right)^4}{\pi c^3 n^3} \begin{cases} F_{n_a\kappa_a}\left(Z_a^{\rm eff}/c\right), & \text{for 1s, 2s, } 2p_{1/2}, \text{ and } 2p_{3/2} \text{ orbotals,} \\ F_{2\kappa_a}\left(Z_a^{\rm eff}/c\right), & \text{for } ns, np_{1/2}, \text{ and } np_{3/2} \text{ orbotals,} \\ 0, & \text{otherwise.} \end{cases} \tag{4}$$

Here, $Z_a^{\rm eff}$ is the effective charge of an electron in orbit a. Diagonal contribution from these vacuum polarization potentials has the form as follows:

$$H_{rr}^{\rm VP} = \sum_{a=1}^{n_w} q_r(a) \int_0^\infty {\rm d}r V^{\rm VP}(r) \left(P_{n_a\kappa_a}^2(r) + Q_{n_a\kappa_a}^2(r)\right). \quad (5)$$

The transition probabilities A_{ij} between the upper state $\Psi_i(\gamma PJM)$ and the lower state $\Psi_j(\gamma' P' J' M)$ can be expressed as

$$A_{ij} = \frac{2\omega}{c} \frac{1}{(2L+1)(2J+1)} \times \left|\left\langle \Psi_j\left(\gamma' P' J' M\right) \left| \tilde{O}^L \right| \Psi_i(\gamma PJM) \right\rangle\right|^2, \quad (6)$$

where $\tilde{O}^L$ is an electromagnetic miltipole transition operator of the order L, ω represents the transition frequency, and c is the light speed in atomic units. For electric dipole and quadrupole (E1 and E2) transitions, there are two forms of the transition operator, i.e., the length (Babushkin) gauge and velocity (Coulomb) gauge. The probability of electric multipole moment transition calculated using a velocity gauge depends mainly on the short range area of the orbital wave function, while the other one depends on the long range area. When using the Racah algebra to obtain the reduced matrix element, the assumption was made that ASFs were built from the same orthonormal radial orbital basis. Since the states of the transitions are always optimized separately to obtain more accurate results, this constraint is severe. This issue can be overcome by transforming the ASFs of the two states of the transitions into biorthonormal terms.[30] The line strength S_{ij} can be defined as

$$S_{ij}^{\rm E2} = \frac{(2J_i+1)\lambda_{ij}^5}{1.11995\times 10^{18}} A_{ij}^{\rm E2}, \quad (7)$$

$$S_{ij}^{\rm M1} = \frac{(2J_i+1)\lambda_{ij}^3}{2.69735\times 10^{13}} A_{ij}^{\rm M1}, \quad (8)$$

where λ_{ij} is the transition wavelength in units of Å.

Furthermore, the lifetime τ of the upper state i can be determined by

$$\tau_i = \frac{1}{\sum_{j,o} A_{ij}^o}, \quad (9)$$

where the notation "o" represents the transition channel from the state i to the state j, and j represents all the states below the state i.

All calculations were performed with the GRASP2K code, provided by Jönsson, Froese Fischer, and Grant *et al.*[31] The GRASP2K package is based on the multiconfiguration Dirac–Hartree–Fock (MCDHF) method. The package consists of a number of application programs and tools to compute approximate relativistic wave functions, energy levels, hyperfine structures (HFS), isotope shifts (IS), Landé g_J-factors, interactions with external fields, angular couplings for labelling purposes, and transition energies and probabilities for many-electron atomic systems.

2.2. Computational model

As shown in Fig. 1, we used several steps to obtain wave functions used in the calculation of transition probabilities. In order to consider the electron correlations sufficiently, the active space approach was used to build the ASFs.[32] According to the perturbation theory, the dominant reference configuration state should be included in the zero-order correlation wave function in Step 1. The set of the first-order ASFs contains all the CSFs obtained by the single and double (SD) substitution of electrons from the occupied orbitals to the virtual orbitals in Step 2, which can be classified according to the substitution of the specific electron pairs.[33] Furthermore, the higher-order set contains the correlations of triple, quadruple or more excitations in Step 3. After considering the Breit interaction and the leading QED effects in MR RCI, the final result of transition probabilities can be calculated using the wave functions in Step 4.

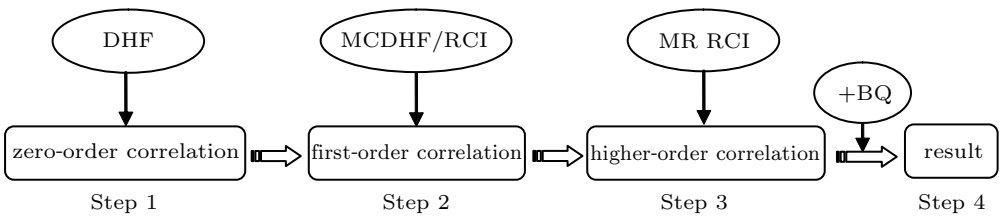


Fig. 1. Calculation steps and corresponding computational methods.

To describe effectively the important zero-order correlations in the first step, we calculated the contributions of the individual electron pairs separately in the DHF. All occupied orbitals were optimized, but kept frozen in the subsequent steps. In this work, $\{1s^2 2s^2 2p^3\}$ was chosen as the reference state for the three concerned $2p^3\ ^4S_{3/2}$, $2p^3\ ^2D_{3/2,5/2}$ states.

The first-order correlation is considered in the MCDHF procedure usually. We devoted to finding a simplified calculation by RCI. In the present work, valence, core–valence, and core–core correlation effects were included. To monitor the convergences of the calculated energies and transition parameters, the active sets were increased in a systematic way by

adding the layers of correlation orbitals. The configuration expansions for the states belonging to $\{1s^2 2s^2 2p^3\}$ were obtained by single-double (SD) excitations to active sets with principal quantum numbers $n \leq 9$ and angular symmetries $l \leq 6$. The amount of computation of MCDHF is quite large if SD excitations including valence, core–valence, and core–core correlation effects go through all the shells. By comparing the MCDHF models of SD excitations including different shells with RCI models containing a diverse combination of wave function and configuration, the important correlation effects in the optimization of orbitals can be differentiated. The amount of computation can be greatly reduced later using appropriate RCI models to obtain the best result. As shown in Fig. 2, ground state energy and transition probabilities of Na^{4+} were calculated. The RCI model 1SCV + CC and the RCI model 1S2SCV + CC can fit the MCDHF model CCCVVV quite well in the calculation of both energy and transition probabilities, which means that the valence and core–valence correlation effects are by far the most important and the core–core effects also come into play at the highest level of accuracy. In consideration of a large computation for model 1S2SCV + CC, we chose the RCI model 1SCV + CC as the optimal substitution calculating the first-order correlations.

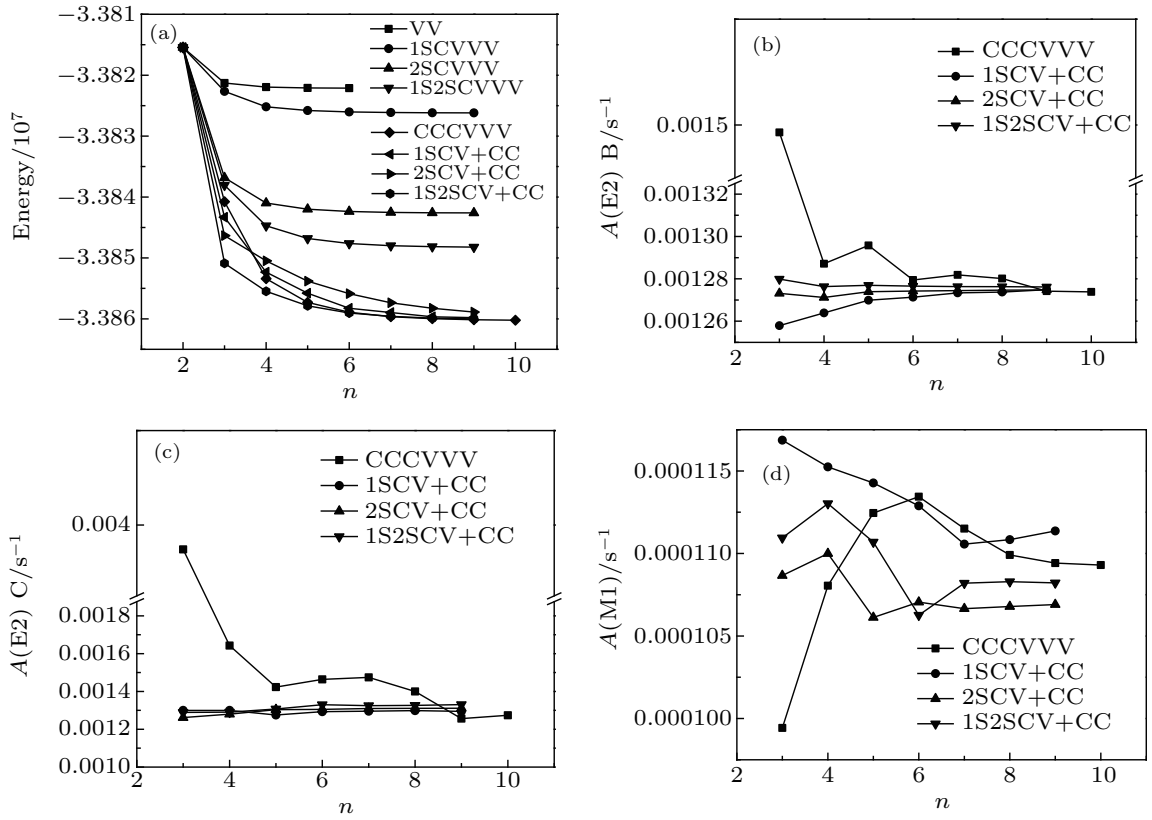


Fig. 2. (a) Ground state energy; (b) transition probabilities of E2 in Babushkin gauge; (c) transition probabilities of E2 in Coulomb gauge; (d) transition probabilities of M1. MCDHF models: VV (valence in 2p), 1SCVVV (valence correlation in 2p and core–valence correlation between 1s and 2p), 2SCVVV (valence correlation in 2p and core–valence correlation between 2s and 2p), 1S2SCVVV (valence correlation in 2p and core–valence correlation between 1s/2s and 2p), CCCVVV (valence correlation in 2p and core–valence correlation between 1s/2s and 2p, core–core correlation between 1s and 2s). RCI models: 1SCV + CC (wave functions from 1SCVVV and configuration from CCCVVV), 2SCV + CC (wave functions from 2SCVVV and configuration from CCCVVV), 1S2SCV + CC (wave functions from 1S2SCVVV and configuration from CCCVVV). Breit interaction and QED effects are out of consideration in the calculation.

The higher-order correlation contains the correlations of triple, quadruple or more excitations. We use the SD excitations of a multireference (MR) approach to involve the important higher-order correlations into the RCI procedure. Then $\{1s^2 2p^5,\ 1s^2 2s 2p^3 3d,\ 1s^2 2\ ^2 2p 3d^2\}$ will be selected as the multireference set. The number of configurations expands up to 6.9×10^5 from 3.0×10^5 in first-order correlations considering a valence correlation for MR. This model is labeled as MR RCI.

Finally, the Breit interaction and the leading QED effects were considered by MR RCI computation, which are labeled as "+B" and "+Q", respectively. E2 and M1 transition probabilities of $2p^3\ ^4S_{3/2}$–$2p^3\ ^2D_{3/2,5/2}$ were computed in the nitrogen-like sequence with $7 \leq Z \leq 16$.

3. Results and discussion

In order to verify the validity of the computational model, we show the calculated forbidden transition probabilities and

excitation energy of Na V of diverse computational models in Table 1, the results of MCDHF and RCI with different principal quantum numbers are also given. With configuration expansion, the calculation difference in excitation energy decreases from 7.45% obtained by DHF to 0.37% obtained by MR RCI, compared with the results obtained from the database of NIST. The final difference from MR RCI + BQ reaches 0.18%, which is in good agreement with that from NIST. The E2 transition probability in the Babushkin gauge is not sensitive to configuration expansion, and the difference between results from DHF and MR RCI is just 4.7%, while the value comes to 65% in the Coulomb gauge. By contrast, Breit interaction exerts an obvious influence on both excitation and transition probabilities, especially for M1 transition probabilities. The value with the Breit interaction is at least 4 times bigger than that without M1, and about 15% smaller for E2 in the Babushkin gauge and 25% or so smaller for E2 in the Coulomb gauge. Excitation energy with adding Breit interaction is obviously smaller than without adding Breit interaction, which is in better agreement with NIST. QED effects come into play at the highest level of accuracy, the value with the QED effect is slightly bigger than without the QED effect for M1 and E2 in the Babushkin gauge, while smaller for E2 in the Coulomb gauge. As for excitation energy, there is no obvious difference.

Table 1. Excitation energies (ΔE in unit of cm^{-1}), M1 transition probabilities (A_{M1} in unit of s^{-1}), and E2 transition probabilities (A_{E2} B and A_{E2} C in unit of s^{-1}) of Na V $^4S_{3/2}$–$^2D_{5/2}$ with diverse computational models. Notations "C" and "B" represent results of A_{E2} in the Coulomb and Babushkin gauges, respectively. A number in a square bracket represents the power of 10. Δ represents the difference between A_{E2} B and A_{E2} C.

	ΔE	A_{M1}	A_{E2} B	A_{E2} C	ΔA^a_{E2}
DHF	51948	6.79[–5]	1.33[–3]	3.76[–3]	64.6%
DHF + B	51870	3.68[–4]	1.12[–3]	3.74[–3]	70.1%
DHF + Q	51948	6.90[–5]	1.34[–3]	3.76[–3]	64.4%
DHF + BQ	51870	3.70[–4]	1.13[–3]	3.74[–3]	69.7%
MCDHF 7	48713	9.60[–5]	1.17[–3]	1.14[–3]	2.5%
MCDHF 7 + B	48624	3.93[–4]	9.96[–4]	8.91[–4]	10.5%
MCDHF 7 + Q	48713	9.73[–5]	1.18[–3]	1.14[–3]	3.4%
MCDHF 7 + BQ	48624	3.95[–4]	1.00[–3]	8.89[–4]	7.1%
MCDHF 9	48656	9.63[–5]	1.17[–3]	1.09[–3]	6.8%
MCDHF 9 + B	48568	3.93[–4]	9.91[–4]	8.46[–4]	14.6%
MCDHF 9 + Q	48657	9.76[–5]	1.17[–3]	1.08[–3]	7.7%
MCDHF9 + BQ	48568	3.96[–4]	9.96[–4]	8.43[–4]	15.6%
RCI7	48590	1.10[–4]	1.28[–3]	1.37[–3]	6.5%
RCI 7 + B	48499	4.46[–4]	10.77[–4]	10.50[–4]	2.5%
RCI 7 + Q	48590	1.12[–4]	1.29[–3]	1.36[–3]	5.15
RCI 7 + BQ	48499	4.49[–4]	10.82[–4]	10.48[–4]	3.1%
RCI 9	48537	1.11[–4]	1.27[–3]	1.29[–3]	1.5%
RCI 9 + B	48445	4.47[–4]	10.72[–4]	9.90[–4]	7.6%
RCI 9 + Q	48537	1.13[–3]	1.28[–3]	1.29[–3]	7.6%
RCI 9 + BQ	48445	4.50[–4]	10.77[–4]	9.87[–4]	8.3%
MR RCI	48523	1.11[–4]	1.27[–3]	1.30[–3]	2.3%
MR RCI + B	48431	4.47[–4]	10.70[–4]	9.89[–4]	7.6%
MR RCI + Q	48523	1.13[–4]	1.28[–3]	1.29[–3]	0.7%
MR RCI + BQ	48431	4.50[–4]	10.75[–4]	9.87[–4]	8.2%
Nist[b]	48343	7.43[–4]	9.82[–4]		
Han[25]		4.39[–4]		10.50[–4]	

[a] $\Delta A_{E2} = |A_{E2}(B) - A_{E2}(C)|/\max(A_{E2}(B), A_{E2}(C))$

[b] The number in NIST given by Merkelis[19] and Froese Fischer.[21]

The results for the excitation energies and the forbidden transition probabilities of the $2p^3\ ^4S_{3/2}$–$2p^3\ ^2D_{3/2,5/2}$ transition in the N-like ions with $7 \leq Z \leq 16$ are presented in Tables 2, 3, and 4. The results of other theoretical calculations are also listed there. The excitation energy and the transition rates A_{M1} and A_{E2} are also consistent with other calculations. What is worth paying attention to is that there is a very big difference in transition rate A_{M1} between a relativistic framework and a non-relativistic framework. Taking transition probabilities of the $2p^3\ ^4S_{3/2}$–$2p^3\ ^2D_{5/2}$NaV for example, the methods of MCHF-BP,[18] MBPT,[19]and MCHF-BP[21] are not in the frame of relativity, which gave relatively large results. Results in this paper are consistent with other calculations in a relativistic framework.

Table 2. Excitation energies (ΔE) of the $2p^3\ ^4S_{3/2}$–$2p^3\ ^2D_{3/2,5/2}$ transition in N-like ions with $7 \leq Z \leq 16$. Label denotes $^4S_{3/2}$–$^2D_{5/2}$ as A, and $^4S_{3/2}$–$^2D_{3/2}$ as B.

ΔE/cm^{-1}		N	O	F	Ne	Na	Mg	Al	Si	P	S
This work	A	19389	26934	34203	41350	48431	55479	62510	69545	76610	83728
	B	19398	26954	34236	41395	48476	55497	62444	69299	76028	82584
Nist	A	19224	26811	34087	41234	48343	55356	62369	69420	76481	83594
	B	19233	26830	34123	41279	48379	55373	62313	69168	75896	82442
Edlén B[11]a	A			34087	41237		55358	62384	69420		83595
	B			34123	41282		55375	62328	69168		82443
Cheng[12]	A			37841	45025	52142	59219	66277	73336	80419	87554
	B			37870	45064	52177	59217	66176	73032	79748	86271
Merkelis[20]	A				40406	47572	54695	61799	68907	76042	83234
	B				40451	47618	54713	61734	68664	75471	82111
Vilkas[21]	A	19022	26698	34030	41212	48315	55378	62422	69461		83656
	B	19029	26718	34062	41256	48361	55398	62362	69226		82540
Fischer[22]	A	19224[b]	26811[b]	34342	41532	48656	55750				
	B	19233[b]	26830[b]	34375	41575	48697	55758				
Wang[24]	A	19350	26923	34207	41382	48489	55592	62643			
	B	19347	26917	34197	41357	48434	55474	62409			
Rynkun[25]	A			34329	41490	48574	55592	62610	69662	76723	83839
	B			34297	41446	48530	55577	62540	69410	76136	82688

[a]: Results from experiments.

[b]: Adjusted data.

Table 3. M1 transition probabilities (A_{M1} in unit of s^{-1}) and E2 transition probabilities (A_{E2} B and A_{E2} C of $2p^3\ ^4S_{3/2}$–$2p^3\ ^2D_{5/2}$ in unit of s^{-1}). Notations "C" and "B" represent results of A_{E2} in Coulomb and Babushkin gauges, respectively. A number in square brackets represents the power of 10.

Transition probabilities	A	N	O	F	Ne	Na	Mg	Al	Si	P	S
This work	M1	4.08[–7]	3.08[–6]	1.83[–5]	9.50[–5]	4.50[–4]	1.04[–3]	4.96[–3]	2.03[–2]	7.36[–2]	2.40[–1]
	E2(B)	8.59[–6]	4.03[–5]	1.44[–4]	4.23[–4]	10.75[–4]	2.46[–3]	5.14[–3]	10.01[–3]	1.85[–2]	3.25[–2]
	E2(C)	8.93[–6]	3.86[–5]	1.33[–4]	3.88[–4]	9.87[–4]	2.30[–3]	4.81[–3]	9.41[–3]	1.84[–2]	3.22[–2]
Garstang[27]	M1				1.8[–4]						
	E2				4.1[–4]						
Zeippen[16]	M1	1.94[–7]	1.83[–6]	1.30[–5]	7.76[–5]	4.05[–4]	1.86[–3]	7.57[–3]	2.78[–2]	9.29[–2]	2.86[–1]
	E2	7.08[–6]	3.64[–5]	1.35[–4]	4.06[–4]	10.50[–4]	2.41[–3]	5.06[–3]	9.90[–3]	1.83[–2]	3.24[–2]
Godefroid[19]	M1	9.122[–7]		3.766[–5]	1.545[–4]	7.164[–4]	2.745[–3]		3.312[–2]		
	E2	5.518[–6]		1.118[–4]	2.865[–4]	9.026[–4]	2.102[–3]		8.823[–3]		
Becker[18]	M1			1.45[–5]	7.97[–5]	3.92[–4]	1.65[–3]	6.72[–3]	2.54[–2]	8.80[–2]	2.79[–1]
	E2			1.25[–4]	3.78[–4]	9.93[–4]	2.29[–3]	4.83[–3]	9.49[–3]	1.76[–2]	3.12[–2]
Merkelis[20]	M1				1.69[–4]	7.16[–4]	2.79[–3]	1.01[–2]	3.41[–2]	1.07[–1]	3.17[–1]
	E2				3.74[–4]	9.82[–4]	2.28[–3]	4.84[–3]	9.54[–3]	1.77[–2]	3.15[–2]
Vilkas[21]	M1	2.27[–7]	1.92[–6]	1.244[–5]	6.926[–5]	3.478[–4]	1.575[–3]		2.375[–2]		
	E2		2.269[–5]								
Fischer[22]	M1	9.71[–7]	7.416[–6]	4.07[–5]	1.880[–4]	7.862[–4]	3.044[–3]				
	E2	6.595[–6]	3.382[–5]	1.305[–4]	3.395[–4]	10.19[–4]	2.353[–3]				
Han[26]	M1	3.93[–7]	3.02[–6]	1.75[–5]	9.19[–5]	4.39[–4]	1.91[–3]	7.57[–3]	2.73[–2]	9.12[–2]	2.81[–1]
	E2(C)	8.79[–6]	3.94[–5]	1.40[–4]	4.11[–4]	10.5[–4]	2.37[–3]	4.99[–3]	9.74[–3]	1.80[–2]	3.17[–2]

Table 4. M1 transition probabilities (A_{M1} in unit of s^{-1}) and E2 transition probabilities (A_{E2} B and A_{E2} C of $2p^3\ ^4S_{3/2}$–$2p^3\ ^2D_{3/2}$ in unit of s^{-1}). Notations "C" and "B" represent results of A_{E2} in Coulomb and Babushkin gauges, respectively. A number in square brackets represents the power of 10.

Transition probabilities	A	N	O	F	Ne	Na	Mg	Al	Si	P	S
This work	M1	1.70[–5]	1.49[–4]	9.66[–4]	5.31[–3]	2.58[–2]	8.60[–2]	3.66[–1]	1.37[0]	4.58[0]	1.38[+1]
	E2(B)	5.69[–6]	2.64[–5]	9.44[–5]	2.77[–4]	7.03[–4]	1.60[–3]	3.31[–3]	6.39[–3]	1.16[–2]	1.98[–2]
	E2(C)	5.90[–6]	2.54[–5]	8.74[–5]	2.54[–4]	6.45[–4]	1.49[–3]	3.11[–3]	6.01[–3]	1.15[–2]	1.96[–2]
Garstang	M1				5.3[–3]						
	E2				2.7[–4]						
Zeippen	M1	1.56[–5]	1.41[–4]	9.36[–4]	5.28[–3]	2.62[–2]	1.16[–1]	4.56[–1]	1.62[0]	5.19[0]	1.51[+1]
	E2	4.59[–6]	2.36[–5]	8.77[–5]	2.64[–4]	6.80[–4]	1.56[–3]	3.25[–3]	6.28[–3]	1.14[–2]	1.95[–2]
Godefroid	M1	1.484[–5]		8.563[–4]	4.744[–3]	2.343[–2]	1.030[–1]		1.462[0]		
	E2	3.365[–6]		7.269[–5]	2.238[–4]	5.867[–4]	1.363[–3]		5.617[–3]		
Becker	M1			1.04[–3]	5.52[–3]	2.64[–2]	1.09[–1]	4.29[–1]	1.54[0]	5.04[0]	1.50[+1]
	E2			8.13[–5]	2.46[–4]	6.45[–4]	1.48[–3]	3.10[–3]	6.02[–3]	1.10[–2]	1.89[–2]
Merkelis	M1				4.73[–3]	2.37[–2]	1.06[–1]	4.20[–1]	1.51[0]	4.87[0]	1.43[+1]
	E2				2.42[–4]	6.34[–4]	1.47[–3]	3.09[–3]	6.01[–3]	1.09[–2]	1.89[–2]
Vilkas	M1	1.246[–5]	1.226[–4]	8.673[–4]	5.02[–3]	2.534[–2]	1.13[–1]		1.597[0]		
	E2		3.486[–5]								
Fischer	M1	1.595[–5]	1.414[–4]	9.391[–4]	5.247[–3]	2.595[–2]	1.148[–1]				
	E2	4.341[–6]	2.209[–5]	8.506[–5]	2.562[–4]	6.624[–4]	1.525[–3]				
Han	M1	1.71[–5]	1.50[–4]	9.65[–4]	5.29[–3]	2.57[–2]	1.12[–1]	4.40[–1]	1.56[0]	5.03[0]	1.48[+1]
	E2(C)	5.82[–6]	2.59[–5]	9.16[–5]	2.69[–4]	6.81[–4]	1.55[–3]	3.23[–3]	6.24[–3]	1.13[–2]	1.94[–2]

Table 5. Excitation energies (ΔE in unit of cm^{-1}), the transition wavelengths λ in unit of nm, total transition probabilities (A in unit of s^{-1}), quality factor Q of the forbidden transition probabilities of the $2p^3\ ^4S_{3/2}$–$2p^3\ ^2D_{3/2,5/2}$ transition in N-like ions with $7 \le Z \le 16$, line strengths (S_{E2}, S_{M1} for E2 and M1), line intensity ratios ($A\ (^4S_{3/2}$–$^2D_{5/2})/A\ (^4S_{3/2}$–$^2D_{3/2})$). A number in square brackets represents the power of 10. (Label denotes $4S_{3/2}$–$2D_{5/2}$ as A and $4S_{3/2}$–$2D_{3/2}$ as B).

		$\Delta E/cm^{-1}$	λ/nm	A	Q	$S_{E2\ B}$	$S_{E2\ C}$	S_{M1}	Ratio
N	A	19388.9	515.76	9.00[–6]	4.06[20]	1.68[–4]	1.75[–5]	1.24[–8]	3.97[–1]
	B	19397.8	515.52	2.27[–5]	1.61[20]	7.40[–5]	7.67[–5]	3.46[–7]	
O	A	26933.7	371.28	4.34[–5]	1.17[20]	1.52[–4]	1.46[–4]	3.50[–8]	2.47[–1]
	B	26953.8	371.01	1.75[–4]	2.89[19]	6.64[–5]	6.37[–5]	1.13[–6]	
F	A	34203.1	292.37	1.62[–4]	3.97[19]	1.65[–4]	1.53[–4]	1.01[–7]	1.53[–1]
	B	34236.6	292.09	1.06[–3]	6.08[18]	7.16[–5]	6.64[–5]	3.57[–6]	
Ne	A	41349.8	241.84	5.18[–4]	1.50[19]	1.87[–4]	1.72[–4]	2.99[–7]	9.27[–2]
	B	41394.7	241.58	5.59[–3]	1.40[18]	8.14[–5]	7.47[–5]	1.11[–5]	
Na	A	48431.4	206.48	1.53[–3]	5.98[18]	2.16[–4]	1.98[–4]	8.81[–7]	5.75[–2]
	B	48476.3	206.29	2.65[–2]	3.45[17]	9.38[–5]	8.61[–5]	3.36[–5]	
Mg	A	55478.6	180.25	3.50[–3]	2.99[18]	2.51[–4]	2.34[–4]	1.35[–6]	4.00[–2]
	B	55496.5	180.19	8.76[–2]	1.19[17]	1.09[–4]	1.01[–4]	7.46[–5]	
Al	A	62509.8	159.97	1.01[–2]	1.17[18]	2.88[–4]	2.70[–4]	4.52[–6]	2.73[–2]
	B	62443.7	160.14	3.69[–1]	3.18[16]	1.25[–4]	1.17[–4]	2.22[–4]	
Si	A	69545.7	143.79	3.03[–2]	4.32[17]	3.30[–4]	3.10[–4]	1.35[–5]	2.20[–2]
	B	69298.8	144.30	1.38[0]	9.48[15]	1.43[–4]	1.34[–4]	6.10[–4]	
P	A	76609.8	130.53	9.21[–2]	1.57[17]	3.75[–4]	3.73[–4]	3.65[–5]	2.01[–2]
	B	76028.3	131.53	4.59[0]	3.12[15]	1.63[–4]	1.62[–4]	1.55[–3]	
S	A	83728.5	119.43	2.73[–1]	5.79[16]	4.23[–4]	4.19[–4]	9.11[–5]	1.97[–2]
	B	82584.2	121.09	1.38[1]	1.13[15]	1.84[–4]	1.82[–4]	3.63[–3]	

The transition probabilities for the ions are summarized in Table 5. Here, the linewidth $\Gamma = 1/(2\pi\tau)$, $Q = \nu/\Gamma$, and ν is the transition frequency. Line strengths for E2 and M1 are denoted as $S_{E2\ B}$, $S_{E2\ C}$, and S_{M1}, and the line intensity ratio $A(^4S_{3/2}$–$^2D_{5/2})/A(^4S_{3/2}$–$^2D_{3/2})$ for the plasma diagnostic process is also given there. According to the definition of Q, we calculate the value and found that it decreases slowly along the sequence. Q values of all ions are larger than 10^{15}. To ensure a shrunken electron cloud size, ions need to be highly charged. So neither N nor O^+ can be selected. Simultaneously, one can see that the line strength increases along the HCI sequence, and choosing a higher line strength is beneficial to the experiment. For a promising candidate of HCI clock, it would be better that the clock transition is located in the optical regime

with high Q value. The transition wavelength should be beyond 200 nm to build appropriate lasers for experiments easily, so the Mg^{5+}, Al^{6+}, Si^{7+}, P^{8+}, and S^{9+} are out of consideration. Considering the manipulation process of the atomic clock experiments, the longer lifetime of the upper state of the clock transition is preferable usually. As for this system, some of the lifetimes of the upper states are quite long, which means that linewidths are too narrow to suit the experiments. As the practical and balanced choice, F^{2+}, Ne^{3+}, and Na^{4+} are recommended. The transitions of all three ions are in the visible light region and lifetimes are suitable for experiments.

4. Conclusions

Out of the interest of the plasma diagnostic process and the candidates of the HCIs clocks, we have investigated the M1 and E2 forbidden transition properties of the fine-structure in $2p^3\ ^4S_{3/2}$–$2p^3\ ^2D_{3/2,5/2}$ state for the N-like ions for $7 \leq Z \leq 16$ with the MCDHF method and configuration interaction calculations. The results of the excitation energies are in good agreement with NIST data. The contributions of the electron correlations, Breit interaction, and the leading QED effects are analyzed. It is shown that the good treatment of electron correlation and inclusion of the Breit interaction are essential for reliably predicting the transition properties for these ions. In choosing candidates for HCI clocks from the N-like ions in $7 \leq Z \leq 16$, F^{2+}, Ne^{3+}, and $Na^{4+}$are recommended out of the overall consideration of the Q factor, the lifetime of the clock state, and the wavelength and linewidth of the lasers for experiments.

References

[1] Hinkley N, Sherman J A and Phillips N B 2013 *Science* **341** 1215
[2] Bloom B J, Nicholson T L and Williams J R 2014 *Nature* **506** 71
[3] Campbell C J, Radnaev A G and Kuzmich A 2012 *Phys. Rev. Lett.* **108** 120802
[4] Derevianko A, Dzuba V A and Flambaum V V 2012 *Phys. Rev. Lett.* **109** 180801
[5] Kielpinski D, King B E and Myatt C J 2000 *Phys. Rev. A* **61** 32310
[6] Yudin V I, Taichenachev A V and Derevianko A 2014 *Phys. Rev. Lett.* **113** 233003
[7] Yu Y M and Sahoo B K 2016 *Phys. Rev. A* **94** 062502
[8] Liu J P, Li C B and Zou H X 2017 *Chin. Phys. B* **26** 103201
[9] Mohan A, Landi E and Dwivedi B N 2003 *Astrophys. J.* **582** 1162
[10] Edlén B 1982 *Phys. Scr.* **26** 71
[11] Edlén B 1984 *Phys. Scr.* **30** 135
[12] Cheng K T, Kim Y K and Desclaux J P 1979 *At. Data Nucl. Data Tables* **24** 111
[13] Clementson J, Beiersdorfer P and Browng V 2011 *Can. J. Phys.* **89** 571
[14] Träbert E, Calamai A G and Gillaspy J D 2000 *Phys. Rev. A* **62** 22507
[15] Träbert E, Heckmann P H and Schlagheck W, *et al.* 1980 *Phys. Scr.* **21** 27
[16] Zeippen C J 1982 *Mon. Not. R. Astron. Soc.* **198** 127
[17] Zeippen C J 1987 *Astronomy & Astrophysics* **173** 410
[18] Becker S R, Butler K and Zeippen C J 1989 *Astronomy & Astrophysics* **221** 375
[19] Godefroid M and Fischer C F 1984 *J. Phys. B: At. Mol. Opt. Phys.* **17** 681
[20] Merkelis G, Martinson I and Kisielius R 1999 *Phys. Scr.* **59** 122
[21] Vilkas M J and Ishikawa Y 2001 *Adv. Quantum Chem.* **39** 261
[22] Fischer C F and Tachiev G I 2004 *At. Data Nucl. Data Tables* **87** 1
[23] Tachiev G I and Fischer C F 2002 *Astronomy & Astrophysics* **385** 716
[24] Wang X L, Chen S H, Han X Y and Li J M 2008 *Chin. Phys. Lett.* **25** 903
[25] Rynkun P, Jönsson P and Gaigalas G 2014 *At. Data Nucl. Data Tables* **100** 315
[26] Han X Y, Gao X, Zeng D L, *et al.* 2014 *Phys. Rev. A* **89** 042514
[27] Garstang R H 1960 *Mon. Not. R. Astron. Soc.* **120** 201
[28] Naqvi A M 1951 "Mutual magnetic interaction in p-electron configurations (with calculations of transition probabilities and astrophysical applications)", Ph. D. thesis (Harvard University)
[29] Dyall K G, Grant I P, Johnson C T, Parpia F A and Plummer E P 1989 *Comput. Phys. Commun.* **55** 425
[30] Olsen J, Godefroid M R, Jönsson P, *et al.* 1995 *Phys. Rev. E* **52** 4499
[31] Jönsson P, He X, Fischer C F, *et al.* 2007 *Comput. Phys. Commun.* **177** 597
[32] Fischer C F, Brage T and Jönsson P 1997 *Computational Atomic Structure: An MCHF Approach* (Bristol and Philadelphia: Institute of Physics Publishing)
[33] Zhou F, Qu Y, Li J and Wang J 2015 *Phys. Rev. A* **92** 052505